Non-Exponential Electron Spin Decay in Indium Arsenide Quantum Dots

Daniel F. Craft

A senior thesis submitted to the faculty of
Brigham Young University
in partial fulfillment of the requirements for the degree of

Bachelor of Science

Dr. John Colton, Advisor

Department of Physics and Astronomy

Brigham Young University

April 2013

ABSTRACT

Non-Exponential Electron Spin Decay in Indium Arsenide Quantum Dots

Daniel F. Craft
Department of Physics and Astronomy
Bachelor of Science

Electron spins in InAs quantum dots have been studied using a pump-probe technique that normally yields the T_1 spin lifetime, the time required for initially polarized electrons to relax and randomize. Using a circularly polarized laser tuned to the wavelength response of the quantum dots, the spins are "pumped" into alignment. After alignment, the spins are detected using a second, linearly polarized "probe" laser. The spin response over time is traced out by changing the delay between the two lasers. In contrast with other samples (bulk GaAs and a GaAs quantum well), where the spin response decays exponentially with time, initial data on the quantum dots has shown an unexpected, exponentially decaying sinusoid. This exponentially decaying sinusoid has a decay constant of 190 ns and oscillation frequency of 4.17 MHz, independent of both temperature and magnetic field.

Keywords: Quantum dots, Quantum computer, electron spin, Kerr rotation, T_1 lifetime

ACKNOWLEDGMENTS

First and foremost, I want to thank my wife, Ashley. This entire project has only been possible through her love, support, and tremendous patience. I also want to thank Dr. John Colton for everything he has taught me and helped me with, a list far too long to write out in its entirety. Finally, I want to thank Dr. Jean-Francois Van Huele and Dr. Joseph Moody for all their help editing and revising this text.

Contents

List of Figures

Chapter 1

Introduction

1.1 Overview

The goal of this research is to better understand the behavior of electron spin in indium arsenide (InAs) quantum dots (QDs). More specifically, we set out to characterize how electron T_1 spin lifetimes in InAs QDs change when exposed to different temperatures and magnetic fields. We attempted to determine if this lifetime is long enough in these, or similar, QDs to be suitable candidates for use as qubits in a quantum computer. The T_1 lifetime is a measure of how long it takes initially aligned electron spins to randomize. In order to measure the spin lifetime of the electrons in a QD, we actually measure the spin polarization of the electrons. We first align the electrons' spins, then allow them to randomize and measure the response.

For other samples this measurement has yielded an exponential decay that can be fit with a lifetime [1]. These lifetimes can range anywhere from fifteen to several thousand nanoseconds [2]. For the QD sample, this process was repeated at a few different magnetic fields ranging from 0 tesla to 2 tesla, and at several different temperatures ranging from 1.5 kelvin to 10 kelvin. To our surprise, the QD sample provided no exponential decay. We instead saw an oscillating decay that

did not seem to depend on magnetic field or temperature. We are as of yet unsure exactly what caused this, but one possibility is outlined in Chapter 3.

To measure the spin polarization of the QDs, we used a two-laser system and a large superconducting magnet. One laser was circularly polarized and caused the spins to be aligned. The second laser was linearly polarized, and was used to measure the spin polarization. While passing through the sample, the second laser experienced an effect known as Faraday rotation. Faraday rotation occurs when a linearly polarized laser passes through a spin-aligned material. The angle of polarization for the laser rotates as the beam passes through the sample. The more polarized the spins in the sample, the more the rotation of the polarization. In other words, by measuring the degree of rotation of the linearly polarized beam, we can determine the spin polarization of the sample.

1.2 Quantum Computing

Electron spin lifetimes may seem like an abstract concept, but many real world applications exist for future technologies. Quantum computing is one of the most interesting potential applications of our research. Quantum computers are fundamentally different from classical computers. Instead of using 1s and 0s, or bits, to do calculations, a quantum computer would use quantum mechanical superposition states to do calculations [3]. These states are called qubits [4], a name derived from "quantum bit." Quantum computers have the potential to do certain kinds of calculations exponentially faster than current, classical computers. Quantum computers may exist in the near future, but much research and technological development must be done before that day.

Quantum computers will have several distinct advantages over classical computers. Perhaps the most famous of these is the ability to factor large numbers quickly [5]. Current computers have classical limitations that make it impossible to factor a large number into its primes within a

reasonable amount of time. This is used to develop difficult-to-break encryption and cryptography keys. With a quantum computer, algorithms are possible that would make factoring large numbers much easier, and therefore could potentially break any modern encryption key [5]. Quantum computers would also be much faster than classical computers at doing such things as solving large systems of linear equations [6] and database searching [7].

While the concept of a quantum computer is magnificent, the reality is difficult to obtain. Some of the difficulties are as follows: one must be able to control a well-defined two-level quantum mechanical state with precision, one must be able to read back that quantum mechanical state with precision, the quantum mechanical state must stay coherent longer than the time required to do a calculation, and one must be able to do all these things in a reasonable temperature and magnetic field [4]. Any two-level quantum state could potentially be used as a qubit, but some are far more practical than others. In this thesis, I will exclusively be discussing electron spin as a potential candidate for a qubit.

Electron spin qualifies because there are two distinct electron spin states. It is a good option because those states can be easily manipulated both optically and magnetically. Another aspect of electron spin that makes it such a strong candidate is that it can be read back optically. For use in a quantum computer, however, one must have many different electron spin states in an ordered row, and be able to control and read all of them, similar to a series of transistors. The superposition of spin-up and spin-down meets the quantum computing requirements, and by using specialized nanostructures called quantum dots [4], electron spin is a viable option as a quantum computing state.

1.3 Electron Spin

The angular momentum of an electron is analogous to the total angular momentum of the Earth. Earth's angular momentum can be thought of as the sum of two things: its angular momentum from revolving around the Sun, and the angular momentum it has from spinning on its own axis. Similarly, atomic electrons have two components to their net angular momentum. Part of that momentum comes from the atomic orbital that they happen to reside in, which is analogous to Earth's momentum of revolving around the sun. The second part of an electron's angular momentum comes from an intrinsic property called spin angular momentum, which is similar to Earth spinning on its axis. Throughout this thesis I will be referring to spin angular momentum simply as spin.

Different particles have different values of spin. Free electrons always have a spin of $\hbar/2$ [8]. This spin is an intrinsic property of electrons and never changes. The direction of the spin can vary (and does vary greatly) but the magnitude is always constant. When electrons are placed in a magnetic field, their spins tend to line up either parallel or anti-parallel (after any precession effects have damped out) to the direction of that field. This is because as spinning charges, their spins can be thought of as equivalent to tiny bar magnets. Anti-parallel alignment requires slightly more energy, leading to an imbalance between the two states. More of the electrons will be aligned parallel to the field than anti-parallel. This slight imbalance creates a net electron spin polarization in the direction of the magnetic field. Mathematically, Polarization $= \tanh(\frac{g\mu_B B}{2k_B T})$, which can be determined from Boltzmann statistics. This polarization is plotted and explained in Fig. 1.1.

The polarization effects shown in Fig. 1.1 only take into account an external magnetic field. Using a laser that has been circularly polarized, and using the right material, we can theoretically increase this to nearly 100 percent polarization. Realistically we are probably getting much less than this. This high level of polarization will begin to randomize immediately back into its initial level of polarization as shown in Fig. 1.1, but this takes some time to occur. The time it takes to do

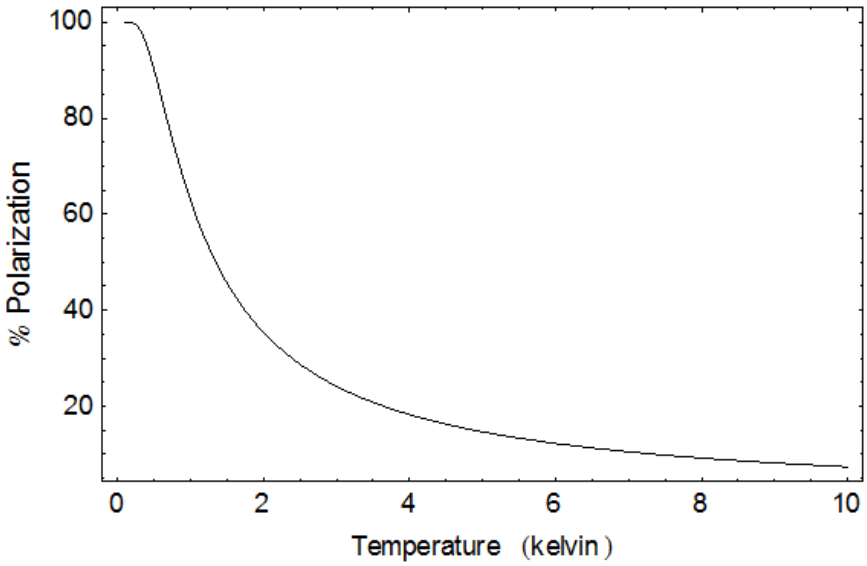

Figure 1.1 Percent polarization as a function of temperature. This plot assumes a magnetic field of 5 tesla in bulk GaAs. Polarization is defined as the percentage of electrons whose spins are parallel to the magnetic field minus the percentage of electrons whose spins are anti-parallel to the magnetic field.

this is characterized by the T_1 spin lifetime, the object of our measurements.

1.4 Photoluminescence in Semiconductors

Before doing any spin lifetime measurements, it is important to perform photoluminescence measurements. Photoluminescence measurements show us what wavelength our sample responds to most, which is the wavelength we set our lasers to in the spin lifetime measurements.

In solids, interacting atomic energy levels in a lattice turn into bands of nearly-continuous energy states [9]. The highest filled energy states make up the valence band, and the lowest unfilled energy states make up the conduction band. The valence and conduction bands are separated by a bandgap in semiconductors and insulators. In metals, the bandgap energy between the valence and conduction bands is virtually non-existant, so they merge into one continuous band. This allows electrical current to flow in metals: their electrons can freely transition from the valence to

conduction bands.

In semiconducting materials, the bandgap energy creates a distinct separation between the valence and conduction bands [9]. Thus, electrons in the valence band are constrained and cannot transition without external energy. If electrons in the valence band absorb sufficiently energetic photons they can transition into the conduction band. When the electrons in the conduction band transition back into the valence band, they emit photons equal to the bandgap energy. This process of optically exciting electrons, then having them fall back via emitted photons, is called photoluminescence (PL).

The specific wavelengths that are emitted during PL allows us to characterize our samples. When we examine the wavelength emitted, we can determine the energy of the bandgap. To do this, we simply shine an intense laser on our sample. The wavelength of the laser must be short enough to ensure that electrons will be excited into the conduction band. Using a spectrometer we can collect light emitted from the sample, and scan across possible wavelengths to determine the entire PL response. For our spin lifetime measurements, we then set our laser wavelength to the peak of our PL response, ensuring we get the most signal possible from our sample. The PL curve for our quantum dot sample is shown in Fig. 1.2, and indicates a peak response at 942 nm.

1.5 Quantum Dots

Quantum dots are tiny nanostructures that are formed when electrons are confined to a 2 nanometer to 10 nanometer spatial region. This can be accomplished by growing two different semiconductors together that have slightly different bandgaps and lattice structures [10]. In the sample we study, those two semiconductors are indium arsenide (InAs) and gallium arsenide (GaAs). When a thin layer of InAs is grown onto GaAs, the InAs buckles to form small isolated regions surrounded by a GaAs barrier layer. Indium arsenide also has a slightly smaller bandgap than GaAs. Because of

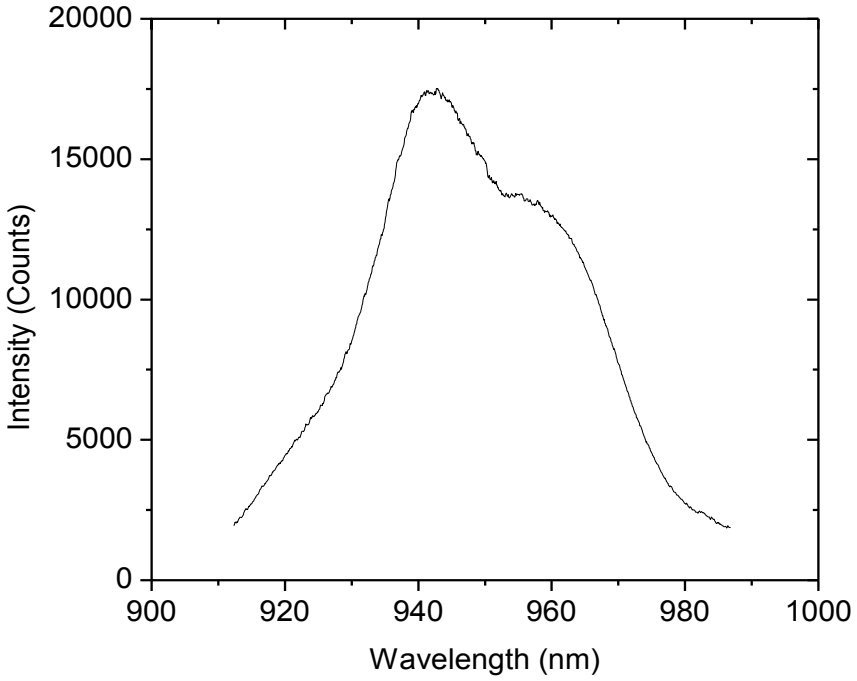

Figure 1.2 The quantum dots exhibit a strong PL response centered at 942 nm. This indicates that more quantum dots have a bandgap equivalent to 942 nm than any other wavelength. We use this knowledge to set our laser wavelength.

this energy difference, an electron that doesn't have quite the energy required to occupy the GaAs conduction band can occupy the InAs conduction band, and becomes confined to the small spatial region defined by the InAs. This energy model of a quantum dot is illustrated in Fig. 1.3. Having performed PL measurements on our quantum dot sample (see Fig. 1.2) we know that the dots exhibit a strong response around 942 nm, indicating that a large number of the dots in the sample have a bandgap equal in energy to 942 nm.

One reason that quantum dots are so interesting is that they have strong potential for quantum computing applications. Electron spins do not stay permanently pointed in the direction they have been left, which is problematic for quantum computing because if the electron spin states random-

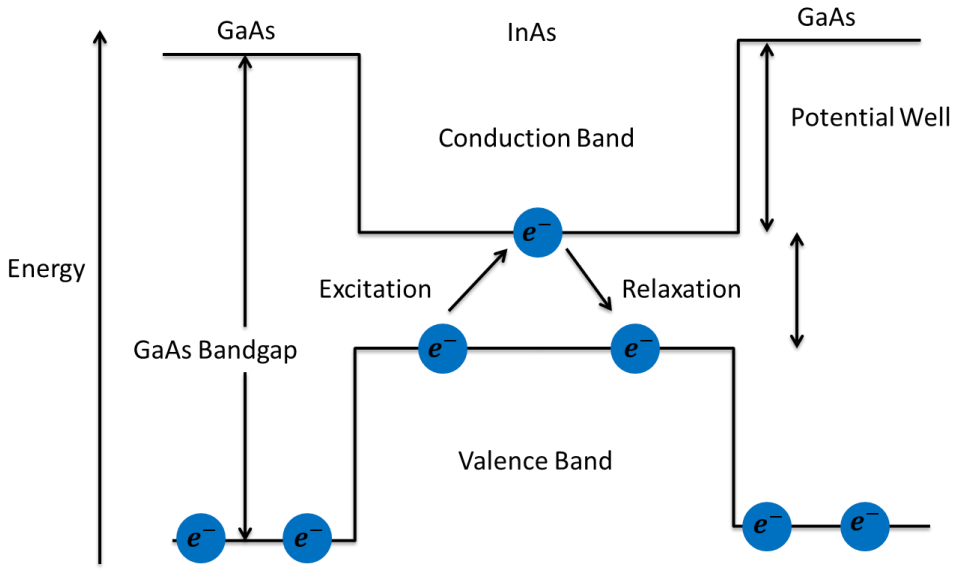

Figure 1.3 Energy model of quantum dots. The energy bands for an InAs quantum dot are shown splitting the (full) valence and (empty) conduction bands of a gallium arsenide barrier, creating a potential well that traps electrons. Excitation and relaxation occur via photon absorption and emission.

ize before a computation is complete, all information contained by those spins will be lost. This means that finding materials that have long spin lifetimes is integral to building a quantum computer. Quantum dots are potentially such a structure, with a relatively long spin lifetime that will be described further in subsection 1.6.2.

1.6 Previous Work

1.6.1 Bulk GaAs and GaAs Quantum Well Lifetimes

Much work has been done with materials and structures related to indium arsenide (InAs) quantum dots that helps us know what to expect from our sample. One such material is bulk gallium arsenide (GaAs). Bulk GaAs experiments have been done on a variety of samples with different doping levels, determining a large range of spin lifetimes. A sample with a doping

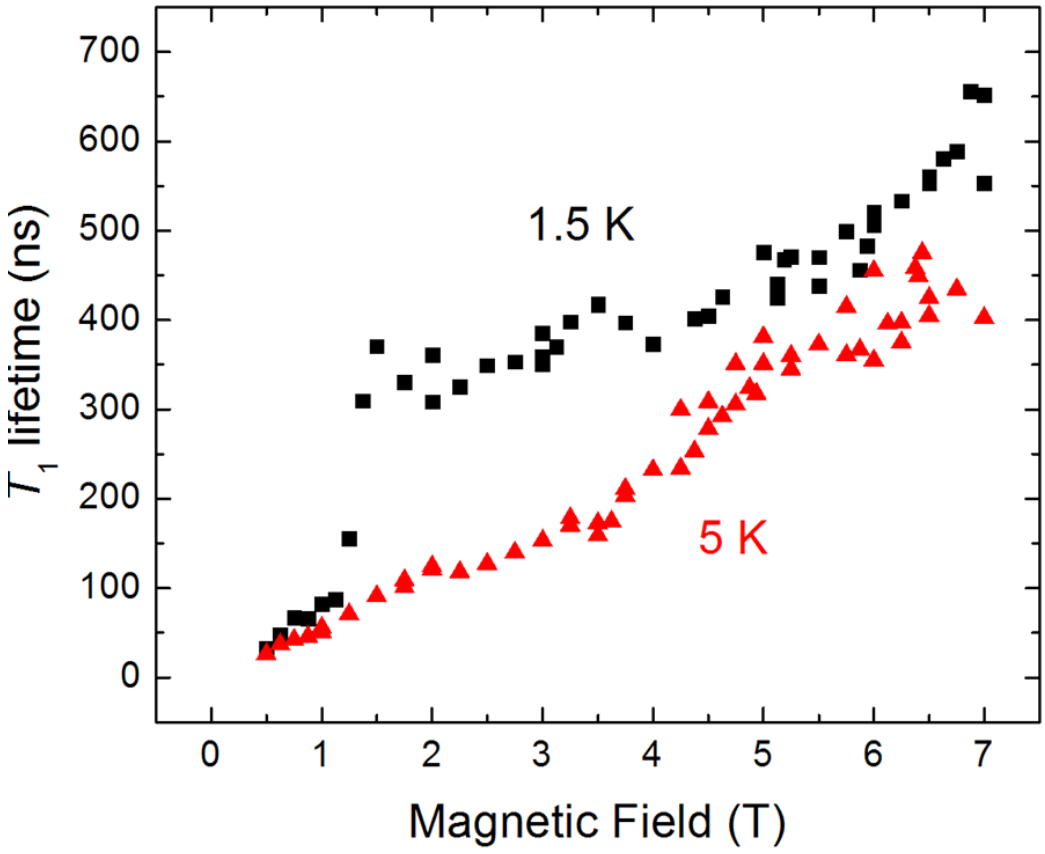

Figure 1.4 Representative lifetimes shown at two different temperatures (1.5 and 5 kelvin) and magnetic fields ranging from 0-7 tesla. All these lifetimes were measured from a bulk GaAs sample [13].

level of $n = 3 \times 10^{15}$ cm^{-3} had spin lifetimes ranging up to 1.4 μs [11], another sample with $n = 1 \times 10^{15}$ cm^{-3} had spin lifetimes as long as 19 μs [12], a third sample with $n = 3 \times 10^{14}$ cm^{-3} had maximum lifetimes of 650 ns [13], and a final sample with doping of $n = 5 \times 10^{13}$ cm^{-3} had millisecond long spin lifetimes [14]. In general the lifetimes in these samples increased with higher magnetic fields, and were lower at higher temperatures (see Fig. 1.4 for a summary of the lifetimes of the $n = 3 \times 10^{14}$ cm^{-3} sample).

Quantum wells have also provided an interesting area of research for spin lifetimes. Quantum wells are similar to quantum dots, but instead of having electrons constrained in all three spatial

dimensions, they have electrons constrained in only one spatial dimension. These structures can be useful stepping stones to understanding the more complicated dot structures. Relatively little work has been done on quantum wells, but Dr. Colton's research group has studied T_1 spin lifetimes of one GaAs quantum well, determining a range of lifetimes from 50 ns to over 1000 ns [1]. Again, the spin lifetimes increased at lower temperatures and higher fields. This sample showed a strong sensitivity to temperature (similar to the bulk GaAs samples studied), with 1.5 K lifetimes usually at least twice as long as lifetimes at 5 K.

1.6.2 Quantum Dot Lifetimes

Theoretical work has indicated that quantum dot spin lifetimes could be much longer than either bulk GaAs or GaAs quantum wells, and this has been supported by experiments into spin decoherence effects [15] (a related, but separate phenomenon to T_1 spin decay). Similarly to GaAs based quantum wells, relatively little work has been done on quantum dot spin lifetimes compared to bulk GaAs. While several groups have studied a different kind of quantum dot, only one single group has directly measured T_1 lifetimes of quantum dots similar to our sample. They measured lifetimes of 20 milliseconds at a magnetic field of 4 tesla and a temperature of 1 kelvin [2].

Chapter 2

Experimental Design of Spin Lifetime Measurements

2.1 Pump-Probe Scheme

2.1.1 Overview of Pump-Probe Scheme

To measure the quantum dots' electron spin lifetime, we use a pump-probe scheme [1] [13]. A standard pump-probe scheme uses two separate beams to manipulate a sample. One of the beams "pumps" the sample into a desired state, and the second beam "probes" the sample to determine the current state. In our case, the pump beam aligns the QDs' electron spins, and our probe beam measures the current level of polarization. We have slightly modified this basic idea. Instead of using two beams with different origins, we split one original beam into two separate beams using a beam splitter. We also control the timing sequences of the experiment differently than most conventional pump-probe experiments do, as will be explained thoroughly in section 2.2. With the original beam split into two separate beams, we can manipulate them independently and treat the system as a conventional pump-probe scheme.

Using a single origin for our two beams allows us to have both beams with the exact same wavelength. Quantum dots have very specific energy levels, so they only interact with very specific wavelengths. Having previously measured the peak of photoluminescence response in our quantum dots to be 942 nm (see Fig. 1.2), we know that specific wavelength is 942 nm. Accordingly, our tunable laser is set to that wavelength in order to interact with the largest number of dots. Also, because both beams are at the same wavelength and our dots respond specifically to that wavelength, we can ensure that both beams are interacting with the same QDs. To get meaningful results, we need to both measure a large number of dots, and ensure that the dots we measure with the probe beam are the same dots affected by the pump beam. If we probed dots that were never pumped we would get data that has nothing to do with the spin decay we are trying to measure.

2.1.2 Pump Beam

The pump beam's purpose is to coherently align a sizable percentage of the electron spins inside the quantum dots. How high that percentage is depends on, among other factors, the laser power we are using. The pump beam is able to align the QDs' electron spins because it is circularly polarized. Circularly polarized light is characterized by its rotating angle of polarization, and can be created by introducing a slight delay into the vertical component of the oscillating electric field that makes up the light relative to the horizontal component. This delay in electric field in the laser is induced by a photo-elastic modulator (PEM). Circularly polarized light is capable of imparting its angular momentum to electrons, and aligning their spins in one direction.

The PEM is also important because it periodically switches from inducing right hand circular polarization to inducing left hand circular polarization. This helps our signal by reducing nuclear polarization effects that have been significant in other experiments [16]. The PEM also allows us to sync up with a lock-in amplifier capable of measuring the component of spin signal at the same frequency as our PEM. This increases the sensitivity of our experiments.

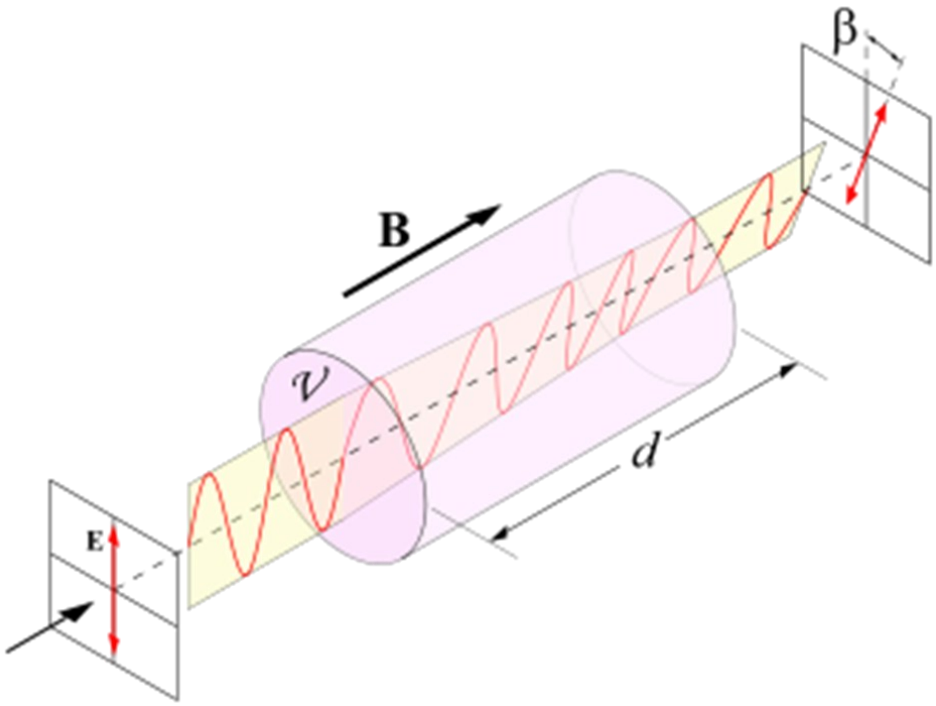

Figure 2.1 Illustration of the Faraday rotation effect. The initial direction of the electric field in this linearly polarized light is vertical. As it passes through a magnetically polarized material the electric field polarization rotates by some angle β. This angle β depends on how magnetically polarized the material is, represented by v, as well as the distance d of the sample that the light passes through. Also notice that for this effect to occur, the magnetic polarization v must be parallel with the propagation direction of the light [17].

2.1.3 Probe Beam

Once the pump beam has aligned the spins, the probe beam can be used to determine their actual level of polarization from Kerr rotation or Faraday rotation. Both effects occur when a linearly polarized laser beam interacts with a magnetically polarized material. It is called Kerr rotation when the beam reflects off the material, and it is called Faraday rotation when the beam passes through the material. After passing through (or reflecting off of) the material, the polarization angle of the laser beam will rotate [13], as shown in Fig. 2.1. The more magnetically polarized a material, the more the laser's polarization angle will rotate. Since the spin polarization is directly

proportional to the Faraday rotation, we can deduce spin lifetimes from changes in the Faraday rotation after passing through the sample.

In order to measure the Faraday rotation of our probe beam, we measure the difference between its vertically and horizontally polarized components. Any angle of linear polarization can be thought of as a linear combination of horizontally and vertically polarized light, and can be split into its vertical and horizontal components using a polarizing beam splitter (PBM).

While keeping the pump laser blocked, which insures our electron spins stay unaligned, we adjust the angle of polarization going into our PBM so that the two components (vertical and horizontal) of our probe laser are equal in intensity. We call this "balancing the beam." We measure a change in balance using a balanced detector that measures the difference in intensity between two beams–the two beams being the two components of the probe beam after passing through the PBM. When balanced, the signal coming from the detector is equal to zero. When the pump laser is unblocked and allowed to pass through the sample, this balance is disrupted because the probe laser has been rotated by Faraday rotation (see Fig. 2.1), leaving its vertical and horizontal components unequal. When all the spins have randomized again the balance will return to zero, because the sample is in the same state it was before ever being pumped. When measuring a spin lifetime, we record the signal from the balanced detector at different times to know how long spin effects persist after initially being pumped.

2.2 Timing

In addition to passing through the PEM, the pump beam passes through an acousto-optic modulator (AOM). The AOM allows us to pulse the pump beam, as well as control when it pulses relative to the probe beam. The probe beam passes through a different AOM, which allows us to independently pulse the two beams, and control their widths and relative delays. This timing is critical.

For the experiments to succeed, we must accurately change the delay between the beams, and we must with equal accuracy correlate the signal from the sample with the specific laser pulse that caused it. One way to reduce noise with this configuration is to cause the two beams to maintain their relative delay through approximately 200 000 periods before moving to a new data point. This allows us to repeat the same data point many times then average it, which reduces noise in the system dramatically.

Using AOMs to control timing is different from using a conventional pump-probe scheme. In a traditional setup, ultrafast laser pulses are used for the pump and the probe pulses, and a mechanical delay line provides the necessary delay between the two pulses. Because these mechanical delay lines are generally very short (typically no longer than several feet), this method is only capable of measuring lifetimes of up to a few nanoseconds. Using an AOM, we can measure lifetimes of up to five thousand nanoseconds, and this limit is not set by the AOMs but by the periodicity of the PEM. Unfortunately, the AOMs that we use have a speed limitation of approximately 20 ns, making it impossible to measure lifetimes shorter than about 35 ns. One other disadvantage of using our two AOMs is that they have a high laser power loss. The AOM that controls the pump beam is the better of the two, with an achievable power throughput of approximately 65 percent. The AOM that controls our probe beam, however, usually only can manage a throughput of around 16 percent. This loss in laser power greatly diminishes the available power for us to use on the sample.

Shown in Fig. 2.2 is a representative spin lifetime scan. This scan was done using a bulk gallium arsenide sample [13], but employed the exact same timing sequence that we used for our quantum dot sample. Examining it will greatly help in understanding the complicated timing involved in these experiments. A two channel pulse generator controls the AOMs for both the pump and the probe beams, and they both have the same period. This period is 4000 ns, which is the same length of time represented in Fig. 2.2 on the x-axis. During one period, both beams pulse

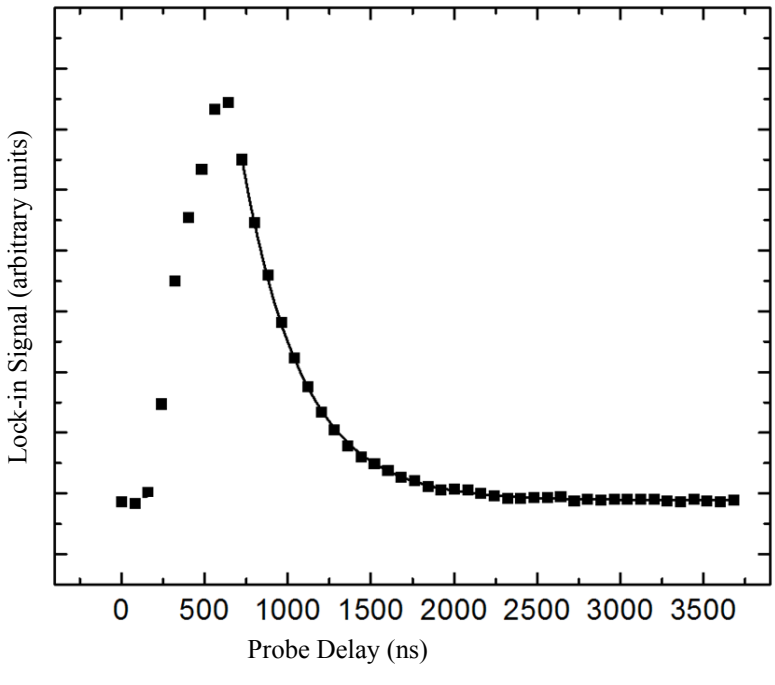

Figure 2.2 Representative spin lifetime scan. Our bulk GaAs sample at 2 T and 1.5 K was fit with an exponential decay to give a T_1 spin lifetime of 359 ns. The pump and probe beams overlap from 250 ns to 750 ns of delay. Everything after 750 ns is true spin decay [13].

once, but at different times. In Fig. 2.2, the pump beam pulse starts at 250 ns delay relative to the beginning of the period (marked 0 ns) and lasts for 400 ns. The probe beam pulse lasts for 100 ns. The pump beam pulse always starts at exactly the same time relative to the start of the period. The pump beam pulse always happens at the same delay, but the relative start time of the probe beam is changed. The x-axis of the plot is labeled probe delay, because it indicates when a pulse from the probe beam reaches the sample relative to the beginning of the period. Each data point in the graph corresponds to a pulse from the probe beam passing through the sample and reaching the detector. For the first few data points, no signal is measured, because the probe beam is arriving at the sample prior to the pump beam. At 250 ns we see an increase in spin polarization, indicating that there is now temporal overlap between the pump and probe pulses. For the next several data

points the spin polarization increases because the amount of temporal overlap between the two beams' pulses is increasing. Finally at 750 ns we see a decrease again, because the two beams' pulses are no longer overlapping in time. This means that any spin polarization that we measure following 750 ns delay (relative to the start of the period) must be coming from spin alignment that is persisting without an external influence, or in other words, it is a true, persisting spin signal.

Due to our periodic timing scheme, some of the data taken is not relevant to spin decay, and is actually part of the initial polarization of the spins caused by the pump laser being currently on the sample. Two methods exist by which we can insure that we examine the correct part of the scan while drawing conclusions about spin decay. First, we must know the widths and delays of both of the beams. For example, in Fig. 2.2, we know that the pump beam has a delay of (meaning it starts to arrive at the sample at) 250 ns, and is 400 ns in width. The probe beam is 100 ns in width. Together that is a width of 500 ns of overlap. So 500 ns after 250 ns, or at 750 ns, they will no longer be overlapping, and the real spin decay begins. Second, we can visually verify what we already suspect will be the case. In the case just mentioned, we calculated that the spin decay should start at about 750 ns. Looking at Fig. 2.2 this is easily confirmed, because it is at 750 ns of delay that the spin polarization starts to decrease. By checking these two methods against each other, we can insure that we are not including any spurious data, and that all our spin lifetimes come from true decay.

2.3 Superconducting Magnet Setup

We perform most experiments with an external magnetic field of at least 1 tesla and a temperature less than 10 kelvin. This requires the use of strong magnets and expensive cryogens. A central focus of the experiment is not just determining a single spin lifetime for QDs, but determining how that lifetime changes according to the surrounding temperature and magnetic field. Gener-

ally speaking, higher temperatures reduce spin lifetimes, and higher magnetic fields increase spin lifetimes (see Fig. 1.4) [1] [13].

For these experiments we used our "blue magnet," a 7 T superconducting magnet. We use this magnet for several reasons. First of all, most of our spin related experiments have been done in this magnet, so we are already very familiar with the setup for it. Also, it can stably achieve temperatures as low as 1.5 K, and can reach magnetic fields up to 7 T. A final advantage with the blue magnet is the direction of the magnetic field that it produces. To measure the potentially long T_1 lifetimes via Faraday rotation, the incoming laser has to be parallel with the magnetic polarization of the sample, which in our case is parallel to the external magnetic field. This alignment is easily accomplished in the blue magnet, because the magnetic field is directed from the front viewing window to the back viewing window, which is exactly where the laser passes through.

Unfortunately, this magnet is expensive to run because the cooling is done with liquid helium. Liquid helium is both expensive to acquire and difficult to store. A 100 liter dewar of liquid helium can keep our magnet running for only a week, so we have to work quickly and efficiently when it is running.

The experimental setup for these experiments requires using many different pieces of optical equipment with precision. The setup used with our blue magnet is shown in Fig. 2.3. As has been explained previously (section 2.1), there are two separate beams that originate from one single laser on the bottom left of the figure. After passing through a power stabilizer the beams are split using a beam splitter. This specific beam splitter is a 9:1 power ratio splitter. The more powerful beam becomes the pump beam, and the weaker beam becomes the probe beam. Both beams pass through AOMs, which are controlled on separate channels in our pulse generator, allowing us to separately pulse them. Once through the AOM, the pump beam is circularly polarized by passing through our PEM, and then both beams are focused with lenses and directed to the sample. We verified the beam diameters of our beams by measuring their beam profiles (see Appendix A). As

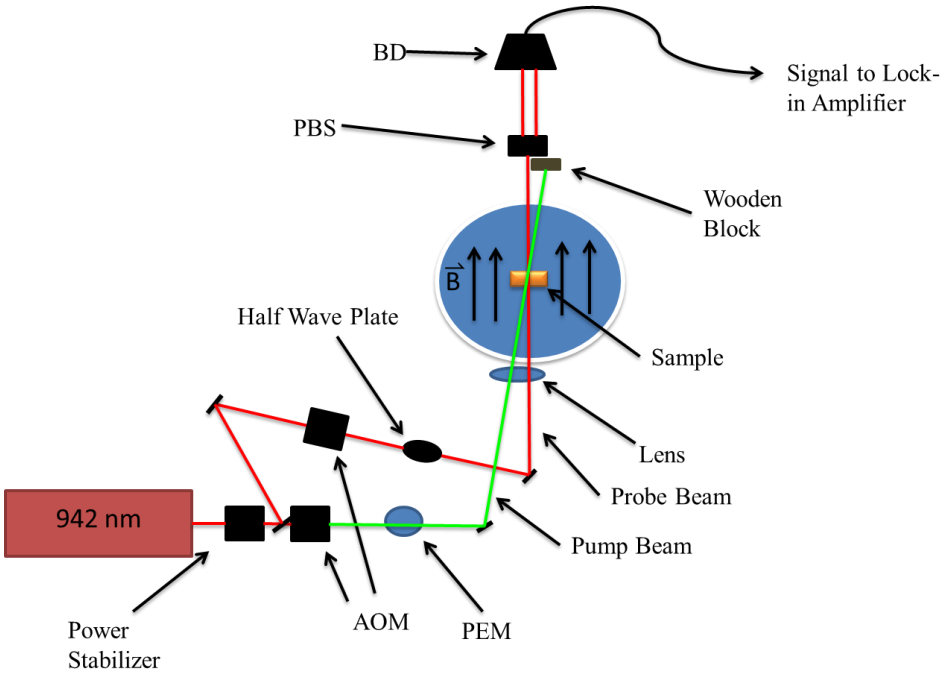

Figure 2.3 Experimental schematic for pump-probe measurements using the superconducting magnet. The pump beam is shown here in green, and the probe beam is red so they can be distinguished easier. Both beams pass through an AOM, and the pump beam passes through the PEM, before reaching the sample. Note that the magnetic field is parallel with the incoming probe laser. After passing through the sample the pump beam is blocked and the probe beam is split with a polarizing beam splitter (PBS). Finally, the probe beam is measured using the balanced detector (BD).

the pump beam passes through the sample the photons impart their angular momentum to the QDs, which aligns their electron spins. When the probe beam passes through the sample, its angle of polarization is rotated via Faraday rotation. The pump beam is blocked on the far side of the sample with a simple, nonreflective, wooden block, while the probe beam passes on to the polarizing beam splitter (PBS). The PBS splits the beam into its horizontally and vertically polarized parts, which then pass into the balanced detector (BD). The signal sent from the BD to the lock-in amplifier is the difference in intensity between the vertically and horizontally polarized components of the probe laser.

Chapter 3

Results and Conclusions

3.1 Expected Results

As has just been explained in Chapter 2, we used a pump-probe scheme to measure spin polarization in an indium arsenide quantum dot sample. Similar experiments have yielded an exponentially decaying behavior for the T_1 lifetime (see Fig. 2.2). The general equation for exponential decay is $y = y_0 + Ae^{-t/\tau}$, where t is time and τ is the decay constant. Fitting the raw data with an exponential decay function gives us the τ decay constant, which is equivalent to the T_1 lifetime [13].

Due to our previous experiments and our experimental setup, we expect our data to show a spin polarization value of zero initially, then a quick increase to a highly positive value as soon as the pump and probe beams overlap. Finally, we expect the spin polarization to start decreasing as soon as the two beams are no longer temporally overlapping. This is all demonstrated succinctly in Fig. 2.2. Due to theoretical considerations [15] and results from other groups [2], we were expecting to measure lifetimes in excess of 1 microsecond at 5 K and 1 T. This would have been significant, as most samples measured have lifetimes considerably shorter than 1 microsecond [1].

In addition to long lifetimes in the sample, we expected to see varying lifetimes as we change

the magnetic field and temperature. In previous samples studied, the spin lifetime has roughly increased as the temperature decreases or as the magnetic field increases (Fig. 1.4). This same general trend was expected for the QD sample.

3.2 Actual Results

When we performed the experiment as has been described, we expected to see the same kind of shape to our scans that was shown in Fig. 2.2, except possibly with longer lifetimes. Instead of simple decays, we observed an oscillating exponential decay with a 190 ns T_1 lifetime and 4.17 MHz oscillation frequency, independent of both temperature and magnetic field.

3.2.1 Overview of Results

Figure 3.1 is a representative plot of what we repeatedly saw. The scan was taken at 5 K and 1 T. Despite its surprising nature, it seems clear that the spin polarization we are measuring is not noise, because it correlates with the pump beam pulse. The oscillations don't start until the pump beam hits the sample. At 250 ns delay relative to the beginning of the period we see signal that becomes a strong positive peak. The highest negative peak at 500 ns delay is the time when the probe beam leaves the pump. This means that all spin signal after that point is persisting without any external pumping. This data is surprising, however, because the signal doesn't just decay exponentially like we would expect, but it decays with oscillations. If the pump beam is no longer aligning the spins, why are they oscillating, and not just decaying? The mathematical fit for this data is shown in Fig. 3.2. The oscillation frequency increases slightly throughout the scan shown in Fig. 3.1 from 3.12 MHz to 5.22 MHz, but is centered at 4.17 MHz. The exponential decay yields a T_1 lifetime of 190 ns.

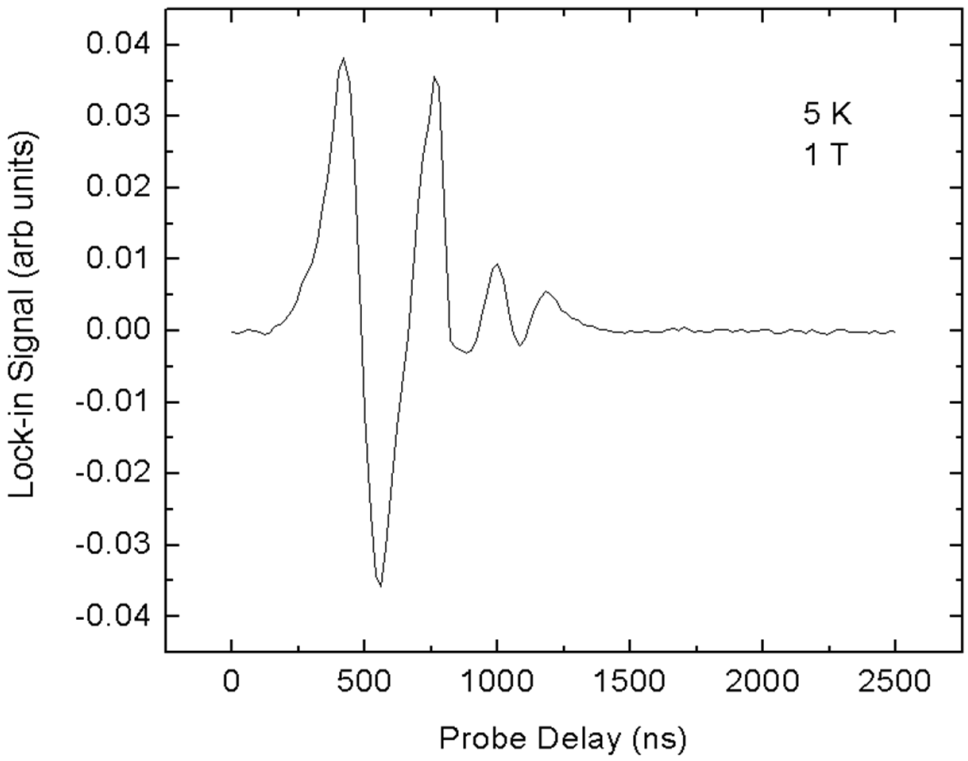

Figure 3.1 Representative pump-probe data for the QD sample. Instead of a simple exponential decay there is an oscillating decay. The pump and probe beams overlap from 250 to 500 ns, which corresponds to the first upslope in the plot and the peak of the primary downward spike, respectively. The spin decay is expected to start after the main down peak at 500 ns. The oscillations decay entirely by 1500 ns delay.

3.2.2 Temperature Dependance of Results

Not only are these oscillations unusual in shape, but they are unusual in how they respond to external conditions. As has been explained in section 3.1, it is expected that the spin lifetime will decrease at higher temperatures. The more energy in the sample, the easier it is for the electrons to flip and randomize. This means that when taking a scan at a higher temperature we expect two things: the overall signal will decrease because there are less electrons initially aligned, and the spins will decay much faster. When we measured the QD sample at 10 K instead of 5 K we did

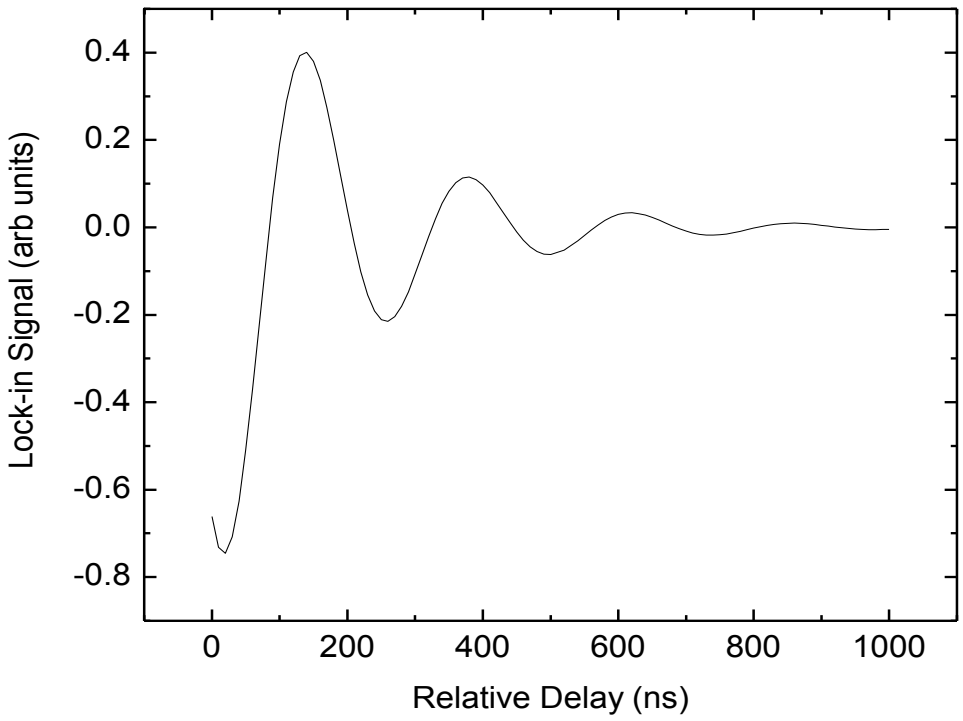

Figure 3.2 Mathematical fit of quantum dot spin polarization data. This fit has a T_1 decay time of 190 ns and a frequency of 4.17 MHz. The *x*-axis corresponds to the 500 ns to 1500 ns range shown in Fig. 3.1.

not observe this expected behavior. We did see a factor of four reduction in overall signal, but the timescale of the plot was entirely unchanged. Figure 3.3 shows two scans taken at two different temperatures. The dashed line and right *y*-axis correspond to the scan shown in Fig. 3.1, and the solid line along with the left *y*-axis corresponds with a scan taken with identical conditions in every way, except the temperature was increased to 10 K. Note that the *y*-axes are on a different scale, indicating the difference in overall spin polarization. The *x*-axis, or time delay, is the same. The two plots show the same behavior, in the same shape, at the same time, regardless of temperature. This is unlike any spin behavior we have previously measured.

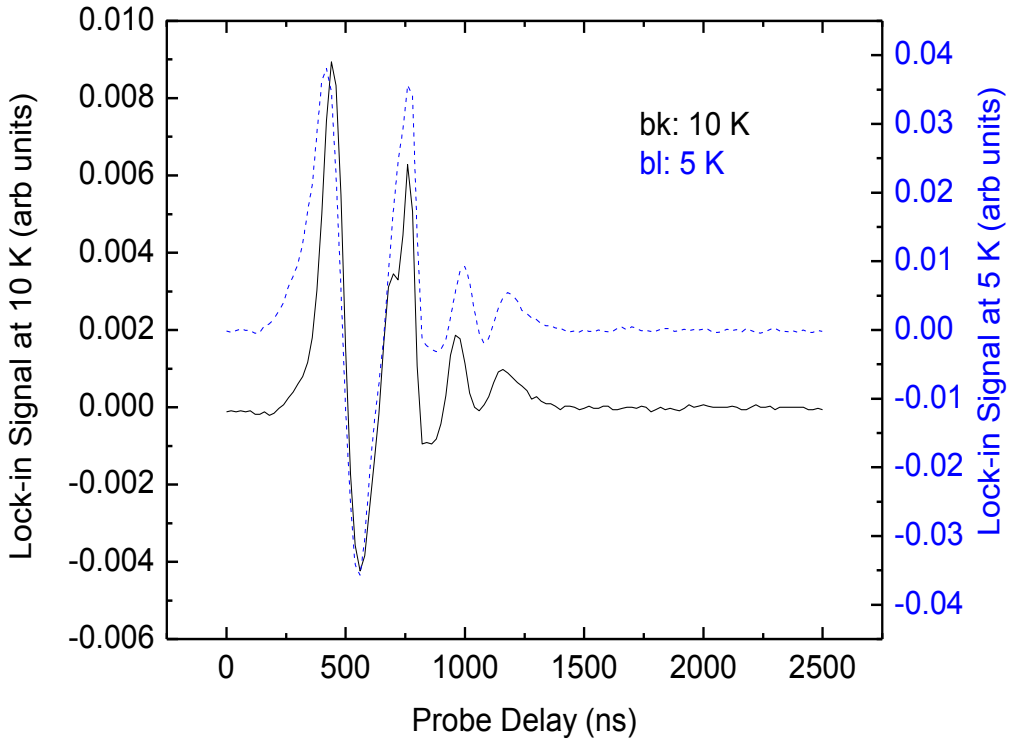

Figure 3.3 Spin polarization response for InAs quantum dots at two different temperatures. The dashed curve represents the same scan that was shown in Fig 3.1, and the solid curve represents a scan taken under the same conditions except the temperature was 10 K instead of 5 K. The x-axis again represents the time delay of the probe beam relative to the beginning of the period. The left side of the graph shows the y-axis for the solid curve in black, and the right side of the graph shows the y-axis for the dashed curve in blue.

3.2.3 Magnetic Field Dependance of Results

Finally, we noted that the spin polarization response was independent of magnetic fields as well as temperature. One of the first theories that we developed was that these oscillations could be caused by spin precession. It is possible to induce and measure spin precession if there is a component of the probe laser that is not completely parallel with the magnetic field. In that case we would see oscillations that correlate with the spin decoherence time of the sample, otherwise known as the T_2^* lifetime [15]. The frequencies in precession oscillations are specific to the type of sample being

studied, but are linearly proportional to the external magnetic field. We knew that it was possible for us to see this effect, because the probe laser was not completely parallel to the magnetic field. The probe beam actually passes through the magnet at a very small angle. We decided to measure if we were in fact seeing precession oscillations by changing the external magnetic field. After taking both scans in Fig. 3.4, however, we determined this was impossible, because the frequency of oscillations did not change even when the magnet was turned off.

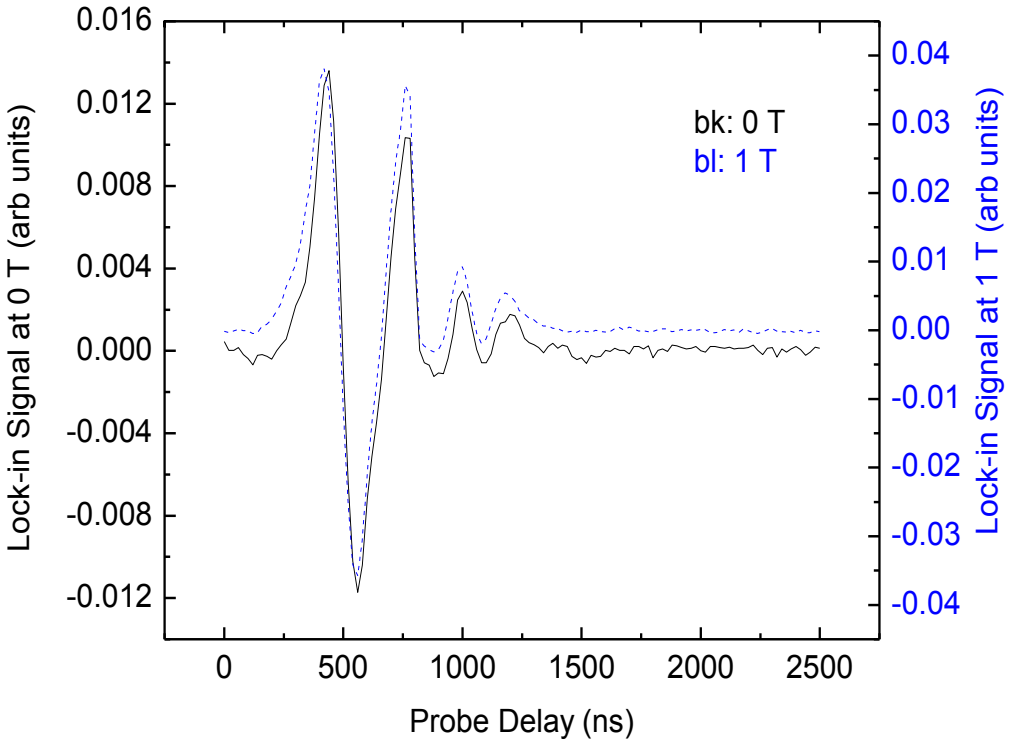

Figure 3.4 Spin polarization response for InAs quantum dots at two different magnetic fields. The dashed curve represents the first scan shown in Fig. 3.1. The solid curve represents a scan with all the same conditions, except an external magnetic field of 0 T instead of 1 T. The *y*-axis on the left represents the solid curve, and the right side scales for the dashed curve. Just like in Fig. 3.2, all major features of the graph are the same except for the absolute scale, which is again much higher for the original, 1 T scan.

3.3 Further Work

Further experiments need to be done to determine the veracity and reproducibility of these results. In future experiments, however, we have decided to attempt a slightly modified setup. In the course of our experiments with quantum dots in our blue magnet we realized that the full capabilities of the magnet were not being realized. We never needed to go higher than 1 T and we never needed to go lower than 5 K. With these lesser constraints, we can use a combination of a closed-cycle cryostat that goes down to 5 K with an electromagnet that goes up to 1 T, instead of using the superconducting magnet (see Fig. 3.4).

A closed-cycle cryostat works by allowing initially cold and compressed helium gas to expand in the presence of a metal rod. The expanding gases remove heat from the rod, cooling it. The gases are then cooled and compressed again, then cycled back through the system. The other end of the rod, called the cold finger, also cools, albeit more slowly [18]. We can optically access the end of the cold finger–where the sample is–through four viewing windows.

There are several reasons to use our cryostat and electromagnet instead of our superconducting magnet. The two together achieve the same conditions as the blue magnet without the use of expensive cryogens, because in a closed-cycle cryostat the helium is never used up, so it does not need to be replaced. Because we don't have to worry about running out of our liquid helium we don't have to rush as much, allowing us to pursue our experiments at a slower pace and without as much expense.

As seen in Fig. 3.5, the setup using the electromagnet and cryostat differs slightly from the more traditional arrangement. As mentioned previously (section 2.1.3), in order to measure T_1 lifetimes using Faraday rotation, the incoming probe beam must be parallel with the magnetic polarization of the sample. In our case, that also means parallel to the externally applied magnetic field. This is easily accomplished in the blue magnet, because the magnetic field is directed through the viewing windows. In the electromagnet, however, this geometry is difficult to obtain. The

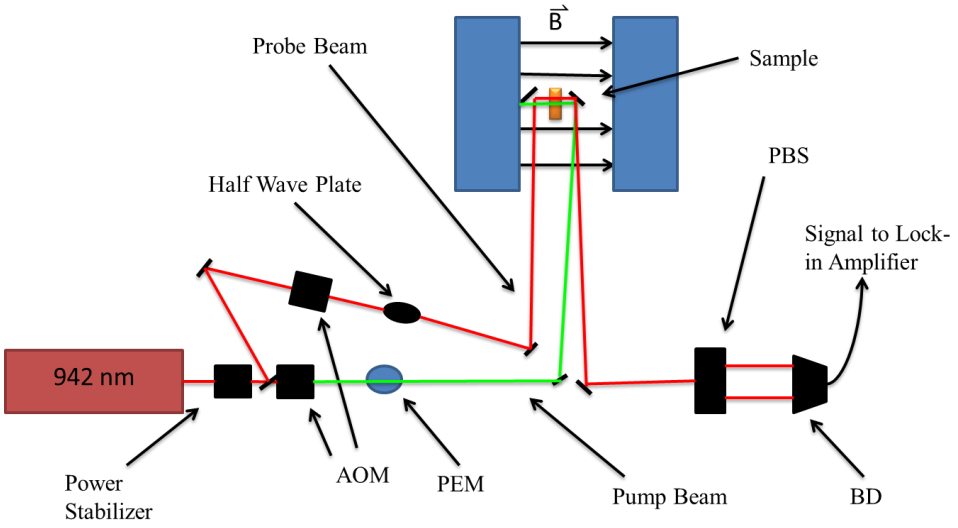

Figure 3.5 Experimental setup for future experiments. The probe beam is shown in red while the pump beam is shown in green for the purpose of distinguishing between them. Note the direction of the magnetic field requires a 90 degree bend in the pump and probe beam paths inside the field region. The pump beam is stopped by hitting one of the magnetic plates, while the probe beam is caught by a second mirror and carried out of the magnet to be split with the polarizing beam splitter (PBS), then measured using the balanced detector (BD).

magnetic field of the electromagnet is directed from one plate to another, so we have to place mirrors next to the magnet to angle the beams in that direction. The issue is exacerbated however, because the sample is in the closed-cycle cryostat (not shown in Fig. 3.5). Even with one mirror placed inside the cryostat, there is less than one centimeter of space for the other mirror to fit between the cryostat and the magnetic plates.

To overcome this challenge we decided to have the pump and the probe beams come from different directions into the sample. As seen in Fig. 3.5, the pump beam approaches the sample from the right, and the probe laser passes through the sample from the left. This separation of the two beams makes it easier to align them both on the sample, and makes it easier to insure that we are not picking up any of the pump beam in our detector.

Despite the difficulties of working with this electromagnet, we have decided to use this method in our future experiments because of the reduced expense when compared to the superconducting magnet.

As soon as we have confirmed our previous measurements, there are several questions to answer. There are three main questions: first, what exactly are these oscillations; second, can the effect be measured and experimented with further; third, is the effect interesting enough to warrant further exploration?

One possibility that deserves to be looked into further is that our probe laser is itself pumping the electron spins. If this is true, the oscillations are indicative of most of the spins switching their spin polarizations coherently, and could be a very interesting phenomenon. This effect is a possible explanation for our results because it is known to produce oscillations, and is independent of magnetic field. To determine if this is indeed the effect, we can alter two things: the laser power, and the pulse width for the pump beam. If the probe beam is causing the polarization to switch and we increase the laser power, the frequency of the oscillations should increase as well. If we adjust the pump beam pulse width the shape of the first oscillation should change because the temporal overlap between the two beams will be different. We will concentrate on these two parameters in further experiments.

3.4 Conclusions

We have observed a never-before-seen spin related effect in our InAs quantum dots. In future studies we will attempt to reproduce this effect, as well as determine the cause of it. The effect's dependence on magnetic field, temperature, laser power, and laser pulse width needs to be characterized. This research will continue to expand our current understanding of quantum dots, electron spin behavior, and the feasibility of future quantum computing technologies.

Appendix A

Beam Profile Measurements

One major difficulty in aligning both beams on the sample is determining the relative size of the two beams when they reach the sample. We are attempting to use the probe beam to measure spin polarization induced by the pump beam, so it is imperative that the probe beam be smaller in diameter than the pump beam. If the probe beam were larger, then we would be measuring spins that were never pumped. To ensure that our probe beam diameter is always slightly smaller than the pump beam diameter, we measure the beam diameters and adjust them as necessary using lenses.

To measure a given beam diameter, we observe how the beam intensity drops as we carefully block the beam with a razor blade attached to a micrometer. We take advantage of the Gaussian intensity distribution of a laser beam in making this measurement. We place our laser power meter behind the razor, and incrementally allow the beam to pass through. At each point we write down the micrometer position and record the laser power from the power meter. After plotting this curve, we take its derivative and fit it with a Gaussian curve of the form shown in Eq. (A.1).

$$y = y_0 + \frac{A}{w\sqrt{\pi/2}} e^{-2\frac{(x-x_c)^2}{w^2}} \tag{A.1}$$

The width constant w in the Gaussian curve corresponds to the diameter of the beam we were

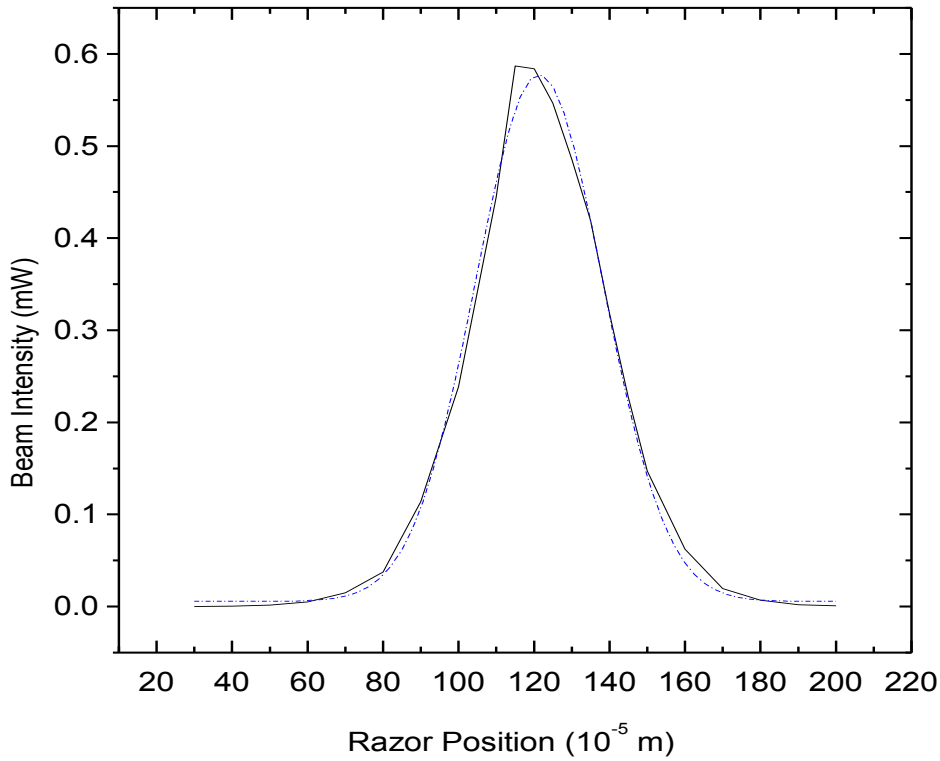

Figure A.1 Beam profile measurements of our probe beam. The solid curve is the derivative of the raw intensity data taken at the indicated micrometer positions. The dashed curve is a Gaussian fit of this curve. Note that the fit is quite good, meaning the laser beam's intensity is almost perfectly Gaussian in shape, as desired. The width constant found in this particular fit indicates the beam measured was 0.33 mm wide in diameter.

measuring. This process is shown in Fig. A.1.

After repeating this process several times, we can extrapolate the exact size of the beam when it reaches the sample. If necessary, we can then adjust the beam diameters by inserting lenses into the beam path. To extrapolate the beam width we use the basic width equation for a focusing or expanding Gaussian beam, $w = w_0\sqrt{1+(z-z_{origin})^2/z_0^2}$, where w is the width of the beam, z is the distance from the focus, z_{origin} is the distance from the narrowest part of the beam to the origin, λ is the laser wavelength, and w_0 is the width of the beam at the narrowest point [19]. Also,

$z_0 = \pi w_0^2/\lambda$, so the only two free parameters are w_0 and z_{origin}. We measured beam diameters at several distances from the sample, then fit the data to the width equation. The resulting theoretical fit with $w_0 = 0.1657$ mm and $z_{origin} = 193$ mm is shown in Fig. A.2 along with the original data points. Using this plot we were able to determine the beam sizes at the sample, and adjust them with lenses as necessary.

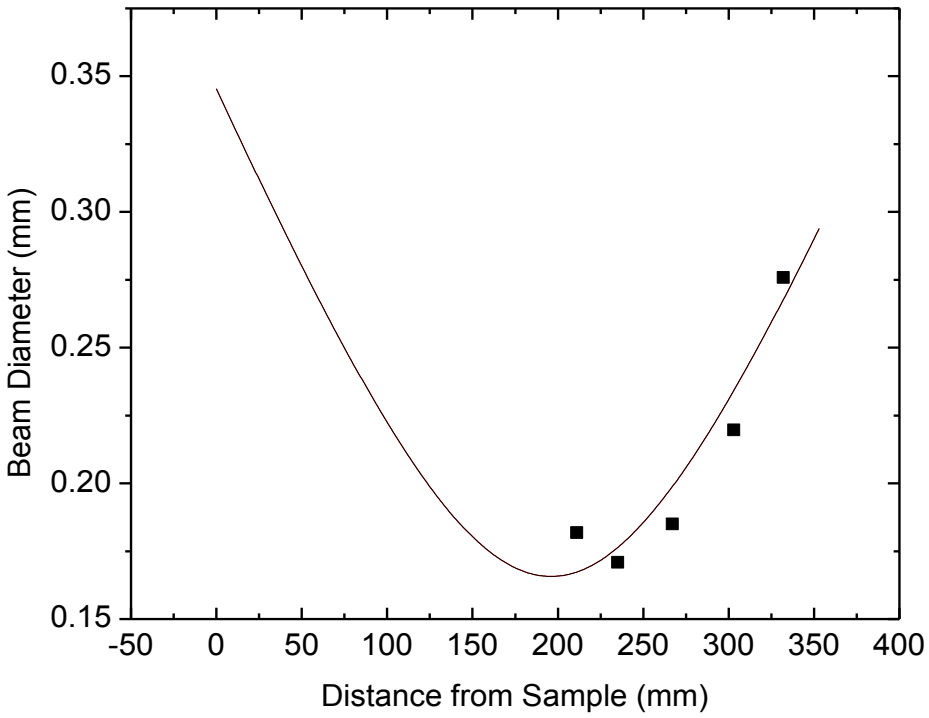

Figure A.2 Summary of beam profile measurements. The squares indicate actual beam profile measurements, and the line shows the theoretical beam width at other distances. Using this plot, we were able to determine that by moving the lens 120 mm we could achieve a beam width of 0.200 mm at the sample. After moving the lens we measured a beam width of 0.2085 mm at the sample, proving the accuracy of our model.

Bibliography

[1] J. S. Colton, D. Meyer, K. Clark, D. F. Craft, J. Cutler, T. Park, and P. White, "Long-lived electron spins in a modulation doped (100) GaAs quantum well," Journal of Applied Physics 112 (2012).

[2] M. Kroutvar, Y. Ducommun, D. Heiss, M. Bichler, D. Schuh, G. Abstreiter, and J. Finley, "Optically programmable electron spin memory using semiconductor quantum dots," Nature **432,** 82 (2004).

[3] A. Steane, "Quantum Computing," Rep. Prog. Phys. 61 (1998).

[4] D. Loss and D. DiVincenzo, "Quantum computation with quantum dots," Phys. Rev. A 57 (1998).

[5] P. Shor, "Algorithms for quantum computation: discrete logarithms and factoring," Proceedings of the 35th Annual Symposium on the Foundations of Computer Science p. 124 (1994).

[6] A. W. Harrow, A. Hassidim, and S. Lloyd, "Quantum Algorithm for Linear Systems of Equations," Phys. Rev. Lett. 103 (2009).

[7] L. Grover, "A fast quantum mechanical algorithm for database search," Proceedings of the 28th Annual ACM Symposium on the Theory of Computing (STOC), p. 212 (1996).

[8] J. R. Taylor, C. D. Zafiratos, and M. A. Dubson, in *Modern Physics for Scientists and Engineers*, 2nd ed., E. Fahlgren, ed., (Pearson Education, Upper Saddle River, NJ, 2004), pp. 287–300.

[9] D. J. Griffiths, *Introduction to Quantum Mechanics*, 2nd ed. (Pearson Education, Upper Saddle River, NJ, 2005), pp. 236–241.

[10] S. Kiravittaya, A. Rastelli, and O. G. Schmidt, "Advanced quantum dot configurations," Rep. Prog. Phys. (2009).

[11] J. S. Colton, T. Kennedy, A. S. Bracker, and D. Gammon, "Microsecond spin-flip times in *n*-GaAs measured by time-resolved polarization of photoluminescence," Phys. Rev. B. 69 (2004).

[12] J. S. Colton, M. E. Heeb, P. Schroeder, A. Stokes, L. R. Wienkes, and A. S. Bracker, "Anomalous magnetic field dependence of the T_1 spin lifetime in a lightly doped GaAs sample," Phys. Rev. B **75,** 205201 (2007).

[13] J. S. Colton, K. Clark, D. Meyer, T. Park, D. Smith, and S. Thalman, "Universal scheme for measuring the electron T_1 in semiconductors and application to a lightly doped n-GaAs sample," Solid State Comm. 152 (2012).

[14] K. M. Fu, W. Yeo, S. Clark, C. Santori, C. Stanley, M. Holland, and Y. Yamamoto, "Millisecond spin-flip times of donor-bound electrons in GaAs," Phys. Rev. B. 74 (2006).

[15] A. Greilich, D. Yakovlev, A. Shabaev, A. L. Efros, I. Yugova, R. Oulton, V. Stavarache, D. Reuter, A. Wieck, and M. Bayer, "Mode Locking of Electron Spin Coherences in Singly Charged Quantum Dots," Science **313,** 341–345 (2006).

[16] B. Heaton, J. Colton, D. Jenson, M. Johnson, and A. Bracker, "Nuclear effects in Kerr rotation-detected magnetic resonance of electrons in GaAs," Solid State Communications **150,** 244–247 (2010).

[17] Wikipedia, "Faraday Effect Picture," (2013).

[18] M. N. Jirmanus, *Introduction to Laboratory Cryogenics* (Janis Research Company Inc., Wilmington, MA., 1990), pp. 50–55.

[19] J. Peatross and M. Ware, *Physics of Light and Optics*, 2011c ed. (available at optics.byu.edu, 2011), pp. 289–290.

Index